

8-1-2001

Coherent control of stimulated Raman scattering using chirped laser pulses

Evan S. Dodd

University of California-Los Angeles, esdodd@ucla.edu

Donald P. Umstadter

University of Nebraska-Lincoln, donald.umstadter@unl.edu

Follow this and additional works at: <http://digitalcommons.unl.edu/physicsumstadter>



Part of the [Physics Commons](#)

Dodd, Evan S. and Umstadter, Donald P., "Coherent control of stimulated Raman scattering using chirped laser pulses" (2001). *Donald Umstadter Publications*. 3.

<http://digitalcommons.unl.edu/physicsumstadter/3>

This Article is brought to you for free and open access by the Research Papers in Physics and Astronomy at DigitalCommons@University of Nebraska - Lincoln. It has been accepted for inclusion in Donald Umstadter Publications by an authorized administrator of DigitalCommons@University of Nebraska - Lincoln.

LETTERS

The purpose of this Letters section is to provide rapid dissemination of important new results in the fields regularly covered by Physics of Plasmas. Results of extended research should not be presented as a series of letters in place of comprehensive articles. Letters cannot exceed four printed pages in length, including space allowed for title, figures, tables, references and an abstract limited to about 100 words. There is a three-month time limit, from date of receipt to acceptance, for processing Letter manuscripts. Authors must also submit a brief statement justifying rapid publication in the Letters section.

Coherent control of stimulated Raman scattering using chirped laser pulses

Evan S. Dodd^{a)} and Donald Umstadter

Center for Ultrafast Optical Science, University of Michigan, Ann Arbor, Michigan 48109

(Received 15 March 2001; accepted 8 May 2001)

A novel method for the control of stimulated Raman scattering and hot electron production in short-pulse laser-plasma interactions is proposed. It relies on the use of a linear frequency chirp in nonbandwidth limited pulses. Theoretical calculations show that a 12% bandwidth will eliminate Raman forward scattering for a plasma density that is 1% of the critical density. The predicted changes to the growth rate are confirmed in two-dimensional particle-in-cell simulations. Relevance to areas of current research is also discussed. © 2001 American Institute of Physics.

[DOI: 10.1063/1.1382820]

High-intensity laser-matter interactions are of much current interest because of their relevance to basic plasma physics, advanced radiation sources,^{1,2} laser-plasma accelerators,^{3,4} laser fusion,⁵ and relativistic nonlinear optics.⁶ Many of these applications depend critically on the amount of laser energy that can be propagated over long distances through plasma without being lost to stimulated Raman scattering (SRS) and electron heating. In the fast ignitor fusion concept, these processes will prevent the high intensity pulse from propagating through the underdense plasma region and will pre-heat the core. In x-ray lasers, which need long gain lengths, electron heating from SRS reduces lasing efficiency.^{7,8} In self-modulated laser-wakefield accelerators, Raman scattering can be either desirable or undesirable, depending on the parameter regime. The laser system used in almost all of these studies is based on the chirped-pulse amplification technique,⁹ which produces large bandwidth light pulses with variable chirp (frequency versus time). Thus, a means to control the growth of SRS by adjustment of the laser chirp could have a significant impact on these applications.

SRS is a process in which light from an incident pump pulse is scattered by the electron-density perturbations of a plasma wave. If the wave has frequency $\omega_e^2 = 4\pi e^2 n/m$, with electron charge e , mass m and number density n and the incident light's frequency is ω_0 , then light will be scattered from noise to frequencies $\omega_1 = \omega_0 - \omega_e$ and $\omega_2 = \omega_0 + \omega_e$,

which are called the Stokes and anti-Stokes lines. The beating between the ω_0 light and that scattered to ω_1 resonantly drives a plasma wave, which creates a feedback loop, since the amount of scattered light is proportional to the plasma wave's amplitude. Therefore, the plasma wave can grow to large amplitudes from noise, scattering light from a seemingly quiet plasma.

The effect of finite-bandwidth on parametric instabilities has been studied extensively.¹⁰ Of the most interest to laser fusion has been bandwidth mismatch. An instability like SRS has an associated bandwidth that the laser bandwidth may exceed. Those frequencies of light outside of the instability bandwidth will then be unable to drive density perturbations, thereby reducing the effective growth rate when $\Delta\omega > \gamma_0$, for growth rate γ_0 and laser bandwidth $\Delta\omega$. Beam smoothing techniques based on spatial and temporal incoherence have also been studied and shown to reduce SRS in experiment.¹¹ Density gradients can also reduce the growth of SRS.¹² Wave breaking saturation has been suggested as a mechanism to control SRS.¹³ However, it only works under specific plasma conditions.

In this paper, we discuss using a linearly chirped pulse to control the reinforcement of density perturbations so as to selectively enhance or eliminate SRS.¹⁴ From the previous discussion on bandwidth mismatch and density gradients, one might think that the growth rate can only be reduced. However, our results will show that the spectral distribution within the pulse is also very important. When group velocity dispersion (GVD) of a chirped pulse is accounted for, the same high bandwidth may either increase or decrease the SRS growth rate. Although others have discussed the idea of

^{a)}Present address: Department of Physics and Astronomy, University of California Los Angeles, Los Angeles, CA 90095-1547; electronic mail: esdodd@ucla.edu

using a chirp,¹⁵ to our knowledge, its effect on SRS has never been examined theoretically. Including the chirp leads to growth rates that differ dramatically from any previous growth-rate calculation. Recent experiments¹⁶ have shown effects similar to what will be presented here analytically and numerically. Chirp has also been shown to affect ionization.¹⁷

The unchirped growth rate has been calculated previously in Refs. 18–20 to be $\gamma_0 = (k_e c / 2\sqrt{2})(\omega_e / \omega_0) a_0$ for Raman forward scattering (RFS) and $\gamma_0 = k_e c / 4(\omega_e / \sqrt{\omega_e \omega_0}) a_0$ for Raman backward scattering (RBS), where $k_e = \omega_e / c$ and $a_0 = e|A| / mc^2$ are the laser pulse's wave number and normalized vector potential. Experiments have recently shown a reasonable agreement with these theoretical calculations of SRS growth.²¹ However, in the following calculation we will use the method of Mori from Ref. 22, instead of a dispersion relation analysis.¹⁸ This newer method includes the dependence of phase and group velocities on longitudinal position within the pulse due to a chirp more intuitively.

The laser pulse interacts with the plasma through the index of refraction as it propagates. Perturbations from electron density, relativistic electron mass and frequency can change the index. The group velocity (v_g) and the phase velocity (v_ϕ), may thus be expanded as

$$v_g = c \left(1 - \frac{1}{2} \frac{\omega_e^2}{\omega_0^2} \left\{ 1 + \frac{\delta n}{n} - \frac{\langle a_0^2 \rangle}{4} - 2 \frac{d\omega_0}{\omega_0} \right\} \right), \quad (1)$$

$$v_\phi = c \left(1 + \frac{1}{2} \frac{\omega_e^2}{\omega_0^2} \left\{ 1 + \frac{\delta n}{n} - \frac{\langle a_0^2 \rangle}{2} - 2 \frac{\delta \omega_0}{\omega_0} \right\} \right), \quad (2)$$

where c is the speed of light, the electron density is n with perturbation δn , and $\delta \omega_0$ represents perturbations to the laser frequency.

The analysis of Ref. 22 starts with the action of the laser pulse, a conserved quantity, and shows that only three types of modulation can occur. These are longitudinal bunching, self-focusing, and photon acceleration, which couple together to form the observed laser–plasma instabilities. Perturbations to the intensity may be written in the form

$$\Delta \langle a_0^2 \rangle = \left\{ -\frac{\Delta L}{L} - 2 \frac{\Delta r_0}{r_0} - \frac{\Delta \omega_0}{\omega_0} \right\} \langle a_0^2 \rangle, \quad (3)$$

where the three terms represent modulation to the: Longitudinal dimension L (bunching), spot size r_0 (self-focusing), and frequency ω_0 (photon acceleration). In the particular case of RFS, a one-dimensional phenomenon with no self focusing, only the two remaining types of modulation contribute. The method relates each type of modulation to dispersion of either v_g or v_ϕ . Longitudinal bunching then becomes $1/L(\partial L / \partial \tau) = -1/c(\partial v_g / \partial \psi)$, and photon acceleration $1/\omega_0(\partial \omega_0 / \partial \tau) = 1/c(\partial v_\phi / \partial \psi)$, in the speed of light frame $\tau = t$ and $\psi = t - z/c$ for pulses propagating in the z direction. By substituting these relations into Eq. (3) an equation describing the growth of RFS was derived. However, instead of rederiving the growth rate, the amount of chirp required to affect the growth of SRS can be estimated.

When a pulse propagates through a dispersive medium it expands or contracts due to GVD of the different frequencies within the pulse, with the bunching rate constant along the length of a linearly chirped pulse. Using the above analysis, in order to eliminate SRS, the bunching rate of the chirp must be equal and opposite to the bunching that drives SRS, or $\partial L_{\text{SRS}} / \partial \tau = -\partial L_{\text{chirp}} / \partial \tau$. Substituting into this the previous relation for bunching, we get

$$L_e \frac{\partial v_g}{\partial \psi} \Big|_{\text{SRS}} = -L_p \frac{\partial v_g}{\partial \psi} \Big|_{\text{chirp}}, \quad (4)$$

the guiding equation for control of SRS through the use of a chirped pulse, where $L_e = 2\pi c / \omega_e$ is the plasma wave length and L_p is the pulse length. Therefore, a pulse undergoing compression will act constructively and reinforce density perturbations, while a pulse that is stretching acts destructively. The GVD due to density perturbations in Eq. (3) is the change in group velocity from peak to trough of the wave. A simple estimate indicates that the required chirp to cancel SRS should have the same Δv_g over $L_e/2$. However, because the bunching rate is uniform over the length of the pulse, Δv_g can be spread out over the entire pulse length, giving the needed bunching rate with a smaller chirp. The two scale lengths L_e and L_p in Eq. (4) act as leverage, amplifying the effect of the chirp.

Laser pulses are not composed of a single frequency, but a spread of frequencies with width $\Delta \omega$ about a central frequency ω_0 . A single frequency only exists as an infinite sine-wave, and any finite length results in more complex spectral content. The Fourier theorem²³ states that any finite signal with root-mean-square (rms) frequency spread Δf_{rms} and length Δt_{rms} must satisfy $\Delta f_{\text{rms}} \Delta t_{\text{rms}} \geq 1/2$. If a pulse with Gaussian profile has a full-width-half-maximum length of τ_p ($L_p = c \tau_p$), then it may be described by an envelope (first exponential) and a carrier (second exponential): $E = E_0 e^{-a\psi^2} e^{i\Phi(\psi)}$, where $\tau_p = \sqrt{2 \log 2/a}$. Along the pulse's length, the frequency may have a sweep or chirp, meaning that frequency may be position dependent. The total instantaneous phase of laser pulse with a linear chirp²³ may be written as $\Phi(\psi) = \omega_0 \psi + b \psi^2$, and the instantaneous frequency $\omega(\psi) = d\Phi/d\psi = \omega_0 + 2b\psi$. The change in frequency along the pulse's length, $\partial \omega / \partial \psi \sim 2b$, perturbs both v_g and v_ϕ , causing the pulse to contract or expand depending on the sign of b . From the GVD dependence on chirp, the effect of the sign will serve to either enhance or reduce the growth of a perturbation. Therefore, a linear chirp can clearly affect the growth of SRS.

Taking Eq. (4) and combining with Eqs. (1) and (2), one finds

$$\begin{aligned} \frac{2\pi}{k_e} \frac{\partial}{\partial \psi} c \left(1 - \frac{1}{2} \frac{\omega_e^2}{\omega_0^2} \left\{ 1 + \frac{\delta n}{n} \right\} \right) \\ = c \tau_p \frac{\partial}{\partial \psi} c \left(1 - \frac{1}{2} \frac{\omega_e^2}{\omega_0^2} \left\{ 1 - 2 \frac{\delta \omega}{\omega_0} \right\} \right). \end{aligned} \quad (5)$$

The change in perturbation size over the length of the pulse is related to the growth, or $\partial / \partial \psi (\delta n / n) \sim \gamma_0$, which can be substituted into the left-hand side of Eq. (5). This is not

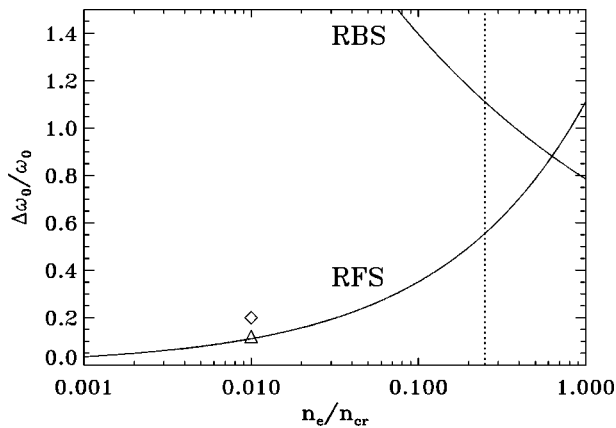


FIG. 1. The amount of bandwidth needed to remove both RFS and RBS is plotted. The triangle represents the 12% bandwidth needed to eliminate RFS at $n/n_{cr} = 1\%$.

meant to be exact but only an approximation to the amount of growth in the perturbations. The chirp perturbation is characterized by $\partial/\partial\psi(\delta\omega/\omega_0) \sim 2b$. These two substitutions yield the desired estimate for the amount of chirp needed to eliminate SRS

$$b = -\frac{1}{4} \frac{\omega_0}{\omega_e} \frac{\gamma_0}{\tau_p}. \quad (6)$$

The bandwidth for a chirped pulse can be written as $\Delta\omega_0 \approx 2b\tau_p$, or $\Delta\omega_0 \approx \frac{1}{2}(\omega_0/\omega_e)\gamma_0$ after substituting in Eq. (6). The use of γ_0 maintains some generality, in that the growth rates for either RFS or RBS may be applied to determine how much bandwidth a chirped laser pulse needs in order to eliminate either instability.

The bandwidth calculated from Eq. (6) is plotted in Fig. 1, for $a_0 = 1.0$, as a function of density proportional to the critical density ($n_{cr} = \omega_0^2 m / 4\pi e^2$). Though the analysis is for $a_0 \ll 1.0$, terms typically appear as $a_0^2/2$, reasonably small for $a_0 \sim 1$. As the plasma density approaches the critical value, the bandwidth required for elimination of RFS grows larger. At $n/n_{cr} \sim 1/4$, ($\gamma_g = 1/\sqrt{1 - v_g^2/c^2} \sim \omega_0/\omega_e = 2$) the bandwidth needed is $\sim 55\%$. But in more underdense regimes, e.g., $\gamma_g \sim 10$, a smaller bandwidth of $\sim 12\%$ is needed to affect propagation, making this concept better suited to these conditions. In the case of direct RBS the amount of bandwidth starts out large, but decreases near the critical density.

Particle-in-cell simulations were run to compare the effect of chirped and unchirped pulses on RFS with the previous calculation. The simulations used the two-dimensional version of the code TRISTAN,²⁴ on eight processors of an IBM SP2. A grid of 1024 by 512 cells was used with 8 particles per cell in a frame co-moving with the pulse. Absorbing boundary conditions were used on all sides so diffracted and scattered light would leave the domain without interfering with the simulation. Three runs were made to study this effect: (A) An unchirped bandwidth-limited pulse with 1.3% bandwidth; (B) negatively and (C) positively chirped pulses, both with 20% bandwidth (~ 200 nm available in Ti:Al₂O₃), instead of 12%. All three were 120 fs half-sine shape pulses with $a_0 = 1.0$, and propagated through $800 \mu\text{m}$ of $n \sim 10^{19} \text{cm}^{-3}$ plasma, where $\omega_0/\omega_e = 10$ for a laser wave-

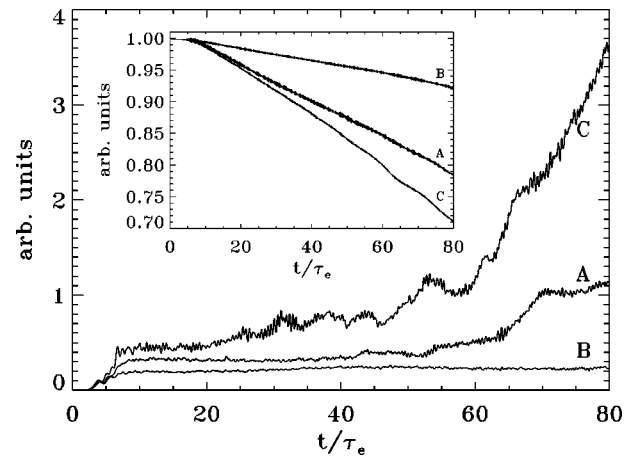


FIG. 2. The main figure shows the amount of energy in the plasma wave as a function of time. The inset shows the energy contained in the laser pulse as a function of time. Both are plotted for: A, an unchirped pulse; B and C, negatively and positively chirped pulses.

length of $1 \mu\text{m}$. This pulse is short enough to drive a small wake that preferentially seeds direct RFS over near-forward RFS. Also, during propagation the pulse length will change only slightly, since $\Delta v_g/c = 0.002$ then $\Delta L/L \sim 4\%$, thus affecting a_0 only slightly.

The total energy of the field components in the simulation is recorded at each time step and the time evolution of the plasma is observed with a fine sampling. In Fig. 2, the total energy in the RFS driven plasma wave is plotted as a function of time τ normalized to the plasma period, τ_e , for the three different runs: A, B, and C. Plotted in each is $\iint (E_x^2/8\pi) dx dy$, where x is the direction of propagation and y is the transverse direction, and should have an exponential growth similar to the wave amplitude. The negatively chirped pulse in B deposits consistently less energy in the plasma wave when compared with the unchirped pulse A, as predicted. The positively chirped pulse in simulation C leads to increased RFS growth, which we see as curve C exceeding A for the entire propagation.

The total energy remaining in the laser pulse is plotted in the inset of Fig. 2. As expected, the negatively chirped pulse, B, maintains the most energy in the pulse, while C experiences the greatest loss in energy, consistent with an increased growth rate. Since the simulation domain is a small box, the pulse will diffract through the boundary, causing an energy loss to the system and there is some heating of the plasma even without RFS. Simulations with a pulse in vacuum and another with only plasma were run to confirm that the shape of the curve B is consistent with energy loss due to diffraction through the boundary. Therefore, qualitatively we see a match between theory and simulation, and that a chirped high-bandwidth pulse can be used to control the growth rate of RFS.

From these diagnostics, the growth rate is found to be reduced, in qualitative agreement with the analytic results. After $800 \mu\text{m}$ of propagation, more than 90% of the light is still in pulse B, compared with under 80% for the unchirped pulse A. The plasma wave in A has saturated at the wave breaking limit, so that the amount of light scattered from such a wave is proportional to the square of the distance

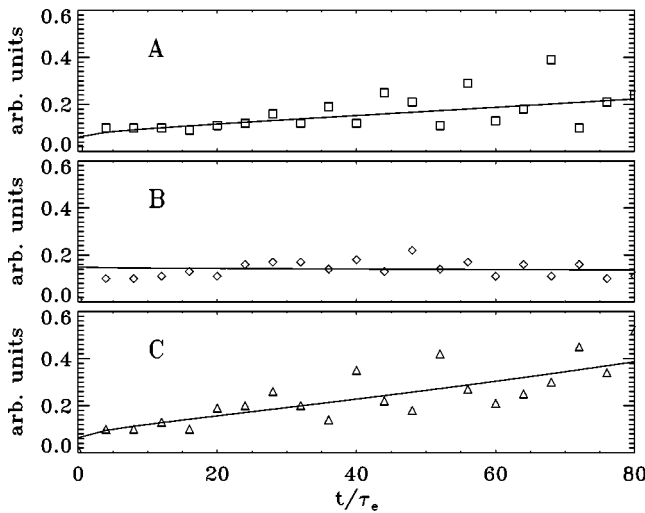


FIG. 3. The amplitude of the density perturbations are plotted as a function of time. Plot A is the unchirped pulse, B, negatively, and C, the positively chirped pulses.

traveled. If the laser pulse had traveled for 1 cm instead of 800 μm , such as in an x-ray laser, the amount of light scattered would be larger by a factor of $(10^4/800)^2 = 156$. Therefore, after 1 cm pulse A would only have 0.5% of its initial energy instead of 80%. Also the growth rate is proportional to a_0 making the growth rate very large at high intensities, such as those required for the fast ignitor concept. In either case, the pulse is expected to propagate many e-foldings of the growth rate, scattering light and heating the plasma if SRS is not controlled.

The density-wave amplitude was directly measured from simulation results saved periodically during each run. In Fig. 3, the wave is seen to grow over time from an initial noise level. The time dependence of the amplitude for short pulse RFS from Ref. 20 is $N = N_0 \exp[\{4\tau \int_{-\infty}^{+\infty} \gamma_0^2(\psi') d\psi'\}^{1/2}] \propto \exp[\alpha\tau^{1/2}]$, for growth rate γ_0 . The integral is performed over the length of the pulse, giving a theoretical value of α , $\alpha_{\text{th}} = 0.18$. A least-square fit is plotted over each run, yielding α for comparison. In A, the rate reasonably matches α_{th} with $\alpha_A = 0.15 \pm 0.07$. The line in B is consistent with a zero growth rate, $\alpha_B = -0.01 \pm 0.04$, as expected. Simulation C gives $\alpha_C = 0.21 \pm 0.06$ which is larger than α_A , but—within the limits of error—is still consistent with the unchirped growth rate. Pulses B and C are identical in all aspects except the chirp and yet their results are remarkably different, illustrating that not only is spectral content important but also its distribution within the pulse.

Fast electron production was also investigated. The maximum oscillation velocity of an electron in the plasma wave for all simulations was just under $\gamma\beta = 1$. Any electron with an energy larger than the maximum oscillation must have been accelerated by the wave. The number of electrons above this value were counted from the simulation and are: $N_A = 5 \times 10^5$, $N_B = 0$ and $N_C = 6 \times 10^7$. We see that not only does a negative chirp reduce the growth of RFS, but it also reduces fast electron production. For the increased growth rate of run C, the number of fast electrons has increased by two orders of magnitude. Therefore, this technique provides

an efficient means of controlling electron production, since the same amount of pulse energy can yield a greater or lesser number of electrons.

We have shown that large chirped bandwidth in a laser pulse can have dramatic effects on the growth of SRS, not just the simple reduction previously predicted for the case of unchirped pulses. The necessary amount of chirped bandwidth for this technique to work was calculated analytically, also showing that the sign of the chirp determines the effect of bandwidth on SRS. These predictions were verified with particle-in-cell simulations of RFS. This technique seems best suited for underdense cases with many e-foldings of the instability, either for large values of the growth rate or where the pulse must propagate long distances. The generation of electrons was also affected, which is critical for the viability of the fast-ignitor, x-ray-laser and wakefield-accelerator concepts.

ACKNOWLEDGMENTS

We thank J.-K. Kim, E. Zeek, T. Neubert, R. P. Drake, and W. Mori for many valuable discussions.

We acknowledge support from Department of Energy award DE-FG02-98ER41071, and the National Science Foundation Center for Ultrafast Optical Science under STC PHY 8920108. Computing services were provided by the University of Michigan CPC, partially funded by National Science Foundation Grant No. CDA-92-14296.

¹R. C. Elton, *X-ray Lasers* (Academic, Boston, 1990).

²J. Workman, A. Maksimchuk, X. Liu, U. Ellenberger, J. S. Coe, C.-Y. Chien, and D. Umstadter, *J. Opt. Soc. Am. B* **13**, 125 (1996).

³T. Tajima and J. M. Dawson, *Phys. Rev. Lett.* **43**, 267 (1979).

⁴D. Umstadter, J. K. Kim, and E. Dodd, *Phys. Rev. Lett.* **76**, 2073 (1996).

⁵M. Tabak, J. Hammer, M. E. Glinsky *et al.*, *Phys. Plasmas* **1**, 1626 (1994).

⁶D. Umstadter and T. B. Norris, *IEEE J. Quantum Electron.* **33**, 1877 (1997).

⁷P. Amendt, D. C. Eder, and S. C. Wilks, *Phys. Rev. Lett.* **66**, 2589 (1991).

⁸S. C. Wilks, W. L. Krueer, A. B. Langdon, P. Amendt, D. C. Eder, and C. J. Keane, *SPIE* **1413**, 131 (1991).

⁹M. D. Perry and G. Mourou, *Science* **264**, 917 (1994).

¹⁰J. J. Thomson and J. I. Karush, *Phys. Fluids* **17**, 1608 (1974); G. Laval, R. Pellat, D. Pesme, A. Ramani, M. N. Rosenbluth, and E. A. Williams, *ibid.* **20**, 2049 (1977); G. Bonnaud and C. Reisse, *Nucl. Fusion* **26**, 633 (1986).

¹¹D. S. Montgomery, J. D. Moody, H. A. Baldis *et al.*, *Phys. Plasmas* **3**, 1728 (1996).

¹²C. S. Liu, M. N. Rosenbluth, and R. B. White, *Phys. Rev. Lett.* **31**, 697 (1973).

¹³P. Sprangle, A. Zigler, and E. Esarey, *Appl. Phys. Lett.* **58**, 346 (1991).

¹⁴E. Dodd and D. Umstadter, *Bull. Am. Phys. Soc.* **44**(7), 244 (1999).

¹⁵R. A. Cairns, D. Johnson, and R. Bingham, *Laser Part. Beams* **13**, 451 (1995); T. M. Antonsen and P. Mora, *Phys. Fluids B* **5**, 1440 (1993).

¹⁶W. P. Leemans, *Bull. Am. Phys. Soc.* **45**(7), 324 (2000); J.-R. Marquès, *ibid.* **45**(7), 325 (2000).

¹⁷B. Rau, C. W. Siders, S. P. Le Blanc, D. L. Fisher, M. C. Downer, and T. Tajima, *J. Opt. Soc. Am. B* **14**, 643 (1997).

¹⁸J. F. Drake, P. K. Kaw, Y. C. Lee, G. Schmidt, C. S. Liu, and M. N. Rosenbluth, *Phys. Fluids* **17**, 778 (1974).

¹⁹N. E. Andreev, L. M. Gorbunov, V. I. Kirsanov, A. A. Pogosova, and A. S. Sakharov, *Plasma Phys. Rep.* **22**, 379 (1996).

²⁰A. S. Sakharov and V. I. Kirsanov, *Phys. Rev. E* **49**, 3274 (1994).

²¹C. Rousseaux, G. Malka, J. L. Miquel, F. Amiranoff, S. D. Baton, and P. Mounaix, *Phys. Rev. Lett.* **74**, 4655 (1995).

²²W. B. Mori, *IEEE J. Quantum Electron.* **33**, 1942 (1997).

²³A. E. Siegman, *Lasers* (University Science, Sausalito, 1986), p. 331.

²⁴J. Villasenor and O. Buneman, *Comput. Phys. Commun.* **69**, 306 (1992).